indicate the shifting pattern of rainfall events in this area. Decrease in rainfall and rainy days will ultimately trigger greater extraction of groundwater for irrigating crops and results in decline of groundwater level. Decrease in rainfall pattern and its variability are likely to reduce soil moisture; while extreme rainfall events in the later monsoon months are likely to increase storm runoff. This accumulated runoff water from adjoining fields of higher elevation poses a serious threat to crops in the depression areas; sometimes it causes total yield losses. Groundwater recharge through artificial groundwater recharge structures installed in low-lying agricultural areas is one of the feasible solutions for controlling flood water damage. Installation of artificial groundwater recharge in these low-lying areas can effectively control excess flood water by draining off excess water into aquifers to improve groundwater recharge and its quality.

1. Christensen, J. H., Regional climate predictions. Climate Change 2007. The physical science basis. Contribution of Working Group 1 to the 4th Assessment Report of the Intergovernmental Panel on Climate Change. Solomon, Cambridge University Press, Cambridge, 2007.
2. Cruz, R. V., Asia. Climate Change 2007. Impacts, adaptation and vulnerability. Contribution of Working Group 2 to the 4th Assessment Report of the Intergovernmental Panel on Climate Change. Cambridge University Press, Cambridge, 2007.
3. Bhadwal, S., Coping with global change: vulnerability and adaptation in Indian agriculture. TERI Report. Venema, IG Printers, New Delhi, 2003.
4. Mooley, D. A. and Parthasarathy, B., Fluctuations in All-India summer monsoon rainfall during 1871–1978. *Clim. Change*, 1984, **6**, 287–301.
5. Parthasarathy, B., Inter-annual and long term variability of Indian summer monsoon rainfall. *Proc. Indian Acad. Sci.* (*Earth Planet. Sci.*), 1984, **93**, 371–385.
6. Rupa Kumar, K., Pant, G. B., Parthasarathy, B. and Sontakke, N. A., Spatial and sub-seasonal patterns of the long-term trends of Indian summer monsoon rainfall. *Int. J. Climatol.*, 1992, **12**, 257–268.
7. Ladha, J. K. *et al.*, How extensive are yield declines in long-term rice–wheat experiments in Asia? *Field Crops Res.*, 2003, **81**, 159–180.
8. Kamra, S. K. and Sharma, D. K., Groundwater recharge structures for small farmers in alluvial regions. Technical Papers, 3rd Ground Water Congress, Central Ground Water Board, Ministry of Water Resources, Government of India, New Delhi, 22–23 March 2011, pp. 168–174.
9. Kumar, S., Kamra, S. K., Yadav, R. K. and Sharma, J. P., Evaluation of sand-based stormwater filtration system for groundwater recharge wells. *Curr. Sci.*, 2012, **103**, 395–404.
10. Choudhury, B. U., Das, A., Ngachan, S. V., Slong, A., Bordoloi, L. J. and Chowdhury, P., Trend analysis of long-term weather variables in mid altitude Meghalaya, North-East India. *J. Agric. Phys.*, 2012, **12**, 12–22.
11. American Public Health Association (APHA), Standard method for examination of water and wastewater, 2002.
12. Guhathakurta, P. and Rajeevan, M., Trends in the rainfall pattern over India, NCC Research Report No 2/2006, India Meteorological Department, Pune, 2006, p. 23.
13. Rupa Kumar, K. *et al.*, High resolution climate change scenarios for India for the 21st century. *Curr. Sci.*, 2006, **90**(3), 334–345.
14. Pattanaik, D. R. and Rajeevan, M., Variability of extreme rainfall events over India during southwest monsoon season. *Meteorol. Appl.*, 2010, **17**, 88–104.
15. Subash, N., Rammohan, H. S. and Sikka, A. K., Quantitative assessment of influence of monsoon rainfall variability on rice production over India. *J. Agrometeorol.*, 2009, **11**, 109–116.
16. Gathala, M. K., Ladha, J. K., Saharawat, Y. S. and Kumar, V., Effect of tillage and crop establishment methods on physical properties of a medium-textured soil under a seven-year rice–wheat rotation. *Soil Sci. Soc. Am. J.*, 2011, **75**, 1851–1862.
17. Kaledhonkar, M. J., Singh, O. P., Ambast, S. K., Tyagi, N. K. and Tyagi, K. C., Artificial groundwater recharge through recharge tube wells: a case study. *Inst. Eng. (I) J. – AG*, 2003, **84**, 28–32.

Raindrop size distributions of southwest and northeast monsoon heavy precipitation observed over Kadapa (14°4′N, 78°82′E), a semi-arid region of India

J. Jayalakshmi[1,2] and K. Krishna Reddy[1,*]

[1]Semi-arid-zonal Atmospheric Research Centre (SARC), Department of Physics, Yogi Vemana University, Kadapa 516 003, India
[2]Department of Physics, Acharya Nagarjuna University, Guntur 522 510, India

Raindrop size distributions (RSD) of southwest (SW – June to September) and northeast (NE – October to December) monsoon heavy precipitation are measured with PARticle SIze and VELocity (PARSIVEL) disdrometer and Micro Rain Radar (MRR) deployed at Kadapa (14.47°N; 78.82°E), a semi-arid continental site in Andhra Pradesh, India. RSD characteristics stratified on the basis of rainrate showed that the mean values of raindrop concentration of small (medium) drops are less (more) in SW when compared with NE monsoon heavy precipitation. Gamma function applied to heavy precipitation events showed that the mean value of mass weighted mean diameter, D_m (normalized intercept parameter $\log_{10} N_w$) is higher (lower) in SW monsoon than NE monsoon. Stratiform and convective precipitating cloud fraction observed during SW and NE monsoons revealed that contribution of stratiform precipitation is predominant for the seasonal variation in raindrop size distribution. The coefficient and exponent values of the $Z–R$ relations are higher in SW than NE monsoon in both stratiform and convective precipitation.

Keywords: Raindrop size distribution, rainrate, mass weighted mean diameter.

*For correspondence. (e-mail: krishna.kkreddy@gmail.com)

IN India, agriculture mainly depends on monsoon rainfall. Andhra Pradesh (AP) is the most disaster-prone area in terms of drought, floods and cyclones. The problem of water shortage in arid zones of AP occurs due to low annual rainfall, excessive temperatures in summer, drastic climatic conditions and the unfavourable distribution of rainfall throughout the year. Based on the agroclimatic conditions, Kadapa experiences nearly 60% of rainfall in southwest (SW) monsoon and more than 30% in northeast (NE) monsoon seasons. Kadapa is located in the central part of Rayalaseema region of AP and its annual average rainfall is much below the national average. Rainfall is an important meteorological parameter, which has direct application to agricultural production and water resources. Monsoon rainfall associated with heavy rainrates may produce natural disasters such as flooding. The precipitation variability is directly allied to the variability of raindrop size distribution (hereafter RSD). The characteristics of such heavy rainfall events can be understood with the help of RSD information. The RSD is related to the rain integral parameters such as rainrate (RR), radar reflectivity (Z) and rain water content (W). Knowledge about RSD will be useful in remote sensing, telecommunications, soil erosion, modelling of clouds and larger scale systems as well as in interpretation of radar and radiometric measurements. Numerous studies on RSD in terms of maritime and continental[1], diurnal, seasonal, intra-seasonal[2–4], different storms[5–7] and rain types[8–10] were conducted across the globe. In India, RSD studies on seasonal[4,11], spatial[12] and cyclonic[13,14] were carried out. Our understanding of the RSD variation, especially, with different heavy precipitation types is still far from complete, and more analyses of *in situ* measurements under a wide variety of climatic regimes are needed. Hence, we have attempted to study RSD characteristics of SW (June to September) and NE (October to December) monsoon heavy precipitation observed in Kadapa, a semi-arid region of India.

The observation site, Yogi Vemana University Campus (14°28′N, 78°42′E, 150 m amsl), is about 15 km from Kadapa city in the southern part of India. RSD are measured using a laser-based disdrometer named PARticle SIze and VELocity (PARSIVEL) disdrometer. Detailed information of the PARSIVEL disdrometer is given by Loffler-Mang and Joss[15] and in brief by Kumar and Reddy[14]. It measures hydrometeors of size ranging from 0.2 to 5 mm for fluid precipitation and 0.2 to 25 mm for solid precipitation and particle velocity ranging from 0.2 to 20 m/s. Micro rain radar (MRR) collocated with PARSIVEL disdrometer is utilized to separate precipitating cloud fractions into stratiform and convective. MRR is capable of providing vertical structure of precipitation and RSD profiles. MRR is a low-cost vertical profiling radar used to determine the enhanced radar reflectivity at zero degree isotherm (bright band)[16,17]. Instrumentations and methodology of MRR can be found in a study by Löffler-Mang

and Kunz[18]. In this study, only heavy precipitation events associated with maximum rainrate value greater than 100 mm/h are considered. The RSD of such heavy precipitation events observed in SW (8568 min) and NE (7020 min) monsoon seasons of 2010 and 2011 are utilized.

The rain drop concentration $N(D)$ (mm^{-1} m^{-3}) at an instant of time from the PARSIVEL disdrometer are obtained from the equation

$$N(D_i) = \sum_{j=1}^{32} \frac{n_{ij}}{A \cdot \Delta t \cdot V_j \cdot \Delta D_i},\qquad(1)$$

where n_{ij} is the number of drops reckoned in the size bin i and velocity bin j, A (m^2) and Δt (s) are the sampling area and time, D_i (mm) the drop diameter for the size bin i and ΔD_i the corresponding diameter interval (mm), V_j (m/s) is the fall speed for the velocity bin j. From the rain drop concentration $N(D)$, drop diameter (D) and fall velocity V_j, the nth order moment of the drop size distribution is expressed as

$$M_n = \int_{D_{min}}^{D_{max}} D^n N(D) \mathrm{d}D,\qquad(2)$$

where n stands for the nth moment of the size distribution.

The one-minute RSD are fitted with gamma function suggested by Ulbrich[19] and is given as

$$N(D) = N_0 D^{\mu} \exp(-\Lambda D),\qquad(3)$$

where D (mm) is the drop diameter, $N(D)$ (mm^{-1} m^{-3}) the number of drops per unit volume per unit size interval, N_0 (mm^{-1} m^{-3}) the number concentration parameter, μ the
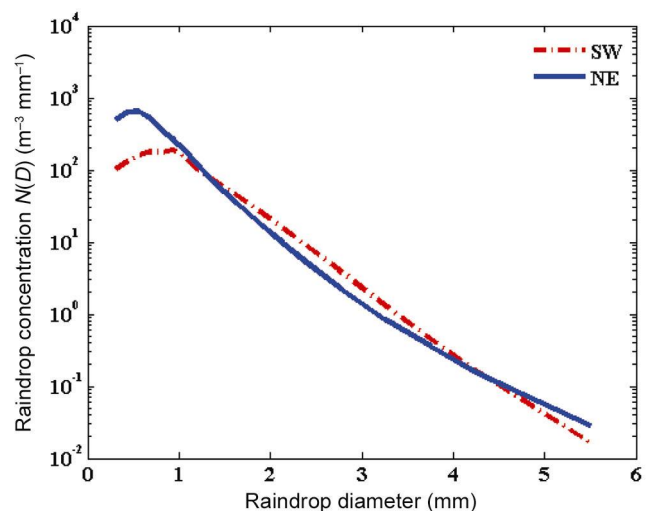
Figure 1. Mean raindrop concentration of SW and NE monsoon heavy precipitation.

Table 1. Statistical measure of disdrometer-derived rainrates (classified into 12 classes) for SW and NE monsoon seasonal raindrop size distribution sets

Rainrate threshold	Class	Southwest (SW) monsoon						Northeast (NE) monsoon					
		n	Maximum (mm/h)	Mean (mm/h)	Standard (mm/h)	Skewness	Kurtosis	n	Maximum (mm/h)	Mean (mm/h)	Standard (mm/h)	Skewness	Kurtosis
$0.1 \le RR < 0.2$	1	1236	0.199	0.145	0.028	0.204	1.892	912	0.199	0.145	0.028	0.135	1.886
$0.2 \le RR < 0.4$	2	1283	0.399	0.289	0.058	0.199	1.806	1080	0.399	0.292	0.057	0.149	1.842
$0.4 \le RR < 0.7$	3	1123	0.699	0.538	0.085	0.139	1.827	1074	0.699	0.539	0.084	0.106	1.888
$0.7 \le RR < 01$	4	730	0.999	0.837	0.087	0.158	1.855	647	0.999	0.841	0.089	0.150	1.773
$01 \le RR < 02$	5	1383	1.998	1.436	0.283	0.265	1.898	1208	1.999	1.444	0.290	0.247	1.871
$02 \le RR < 04$	6	1134	3.999	2.807	0.560	0.408	2.040	965	3.999	2.808	0.554	0.431	2.018
$04 \le RR < 07$	7	599	6.989	5.347	0.867	0.202	1.825	469	6.983	5.227	0.874	0.422	1.931
$07 \le RR < 10$	8	316	9.995	8.409	0.838	0.198	1.919	191	9.915	8.222	0.850	0.465	2.031
$10 \le RR < 20$	9	335	19.947	13.879	2.932	0.521	2.055	222	19.870	13.633	2.716	0.630	2.248
$20 \le RR < 30$	10	146	29.896	24.689	2.814	0.110	1.777	91	29.933	24.452	2.971	0.280	1.896
$30 \le RR < 50$	11	146	49.976	38.764	5.763	0.249	1.821	82	49.473	38.862	5.222	0.345	2.238
$RR \ge 50$	12	137	151.165	79.174	24.285	0.977	3.216	79	177.195	86.740	31.806	1.029	3.425
All		8568	151.165	4.384	11.882	5.9158	46.678	7020	177.195	3.610	10.963	7.839	82.216

Table 2. Mean values of mass weighted mean diameter and gamma parameters at different rainrate classes of SW and NE monsoon heavy rainfall

Rainrate threshold	Southwest (SW) monsoon						Northeast (NE) monsoon					
	D_m (mm)		$\log_{10}(N_w)$ (m^{-1} mm^{-3})		μ (−)	Λ (mm^{-1})	D_m (mm)		$\log_{10}(N_w)$ (m^{-1} mm^{-3})		μ (−)	Λ (mm^{-1})
	Mean	Standard	Mean	Standard	Mean	Mean	Mean	Standard	Mean	Standard	Mean	Mean
$0.1 \le RR < 0.2$	1.01	0.304	3.774	0.441	19.398	24.989	0.86	0.293	4.143	0.645	18.959	28.794
$0.2 \le RR < 0.4$	1.09	0.280	3.873	0.478	15.512	19.318	0.91	0.334	4.330	0.650	15.252	23.675
$0.4 \le RR < 0.7$	1.14	0.305	4.030	0.465	12.940	16.128	0.94	0.291	4.504	0.675	12.477	19.747
$0.7 \le RR < 01$	1.19	0.271	4.103	0.456	11.821	14.311	0.95	0.273	4.658	0.605	12.362	19.023
$01 \le RR < 02$	1.29	0.271	4.130	0.426	9.927	11.697	1.02	0.311	4.734	0.624	11.142	16.855
$02 \le RR < 04$	1.41	0.305	4.209	0.436	7.779	9.039	1.09	0.331	4.862	0.620	10.538	15.038
$04 \le RR < 07$	1.49	0.319	4.359	0.435	6.389	7.479	1.20	0.403	4.925	0.587	10.568	13.524
$07 \le RR < 10$	1.54	0.276	4.467	0.351	5.466	6.488	1.25	0.309	4.985	0.403	10.773	12.447
$10 \le RR < 20$	1.66	0.331	4.507	0.374	6.241	6.457	1.39	0.325	4.939	0.432	8.252	9.355
$20 \le RR < 30$	1.81	0.365	4.549	0.385	5.138	5.241	1.70	0.365	4.701	0.450	6.665	6.493
$30 \le RR < 50$	2.00	0.327	4.485	0.357	3.169	3.699	1.84	0.301	4.697	0.355	4.990	5.081
$RR \ge 50$	2.06	0.248	4.710	0.268	2.026	2.986	2.07	0.252	4.724	0.250	2.352	3.157
All	1.28	0.378	4.101	0.495	11.523	14.130	1.034	0.376	4.595	0.669	12.655	18.842
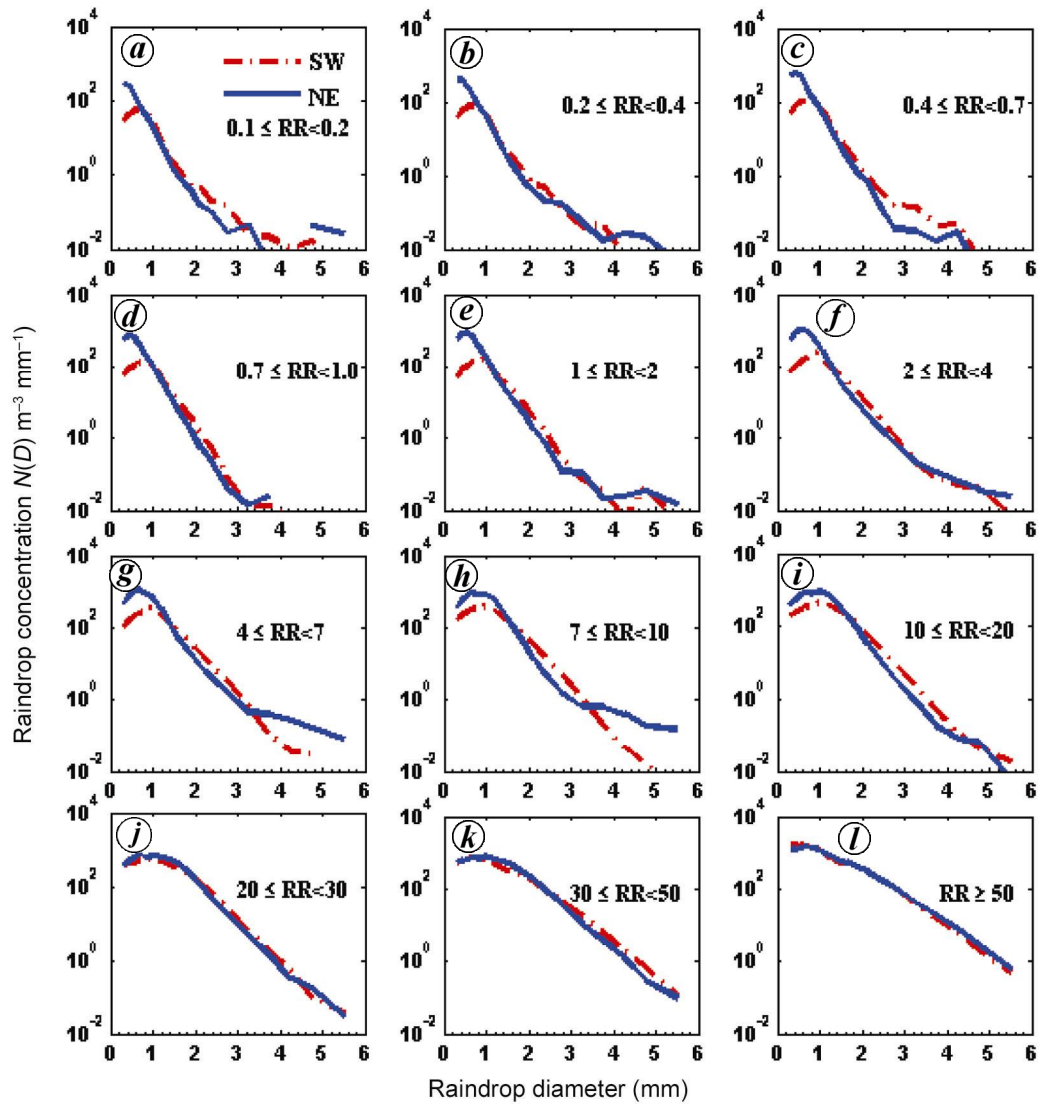
Figure 2. Rate size distribution of SW and NE monsoon heavy precipitation for different rainrates.

shape parameter and Λ (mm^{-1}) is the slope parameter. The mass-weighted mean diameter D_m (mm), shape parameter μ and slope parameter Λ (mm^{-1}) are evaluated from the 3rd, 4th and 6th moments of the size distribution.

$$D_m = \frac{M_4}{M_3}. \tag{4}$$

The normalized intercept parameter N_w (mm^{-1} m^{-3}) defined by Bringi et al.[20]

$$N_w = \frac{4^4}{\pi \rho_w} \left(\frac{10^3 W}{D_m^4} \right), \tag{5}$$

where ρ_w (1 g/m^3) represents the density of water and W (g/m^3) represents the liquid water content for the corresponding size distribution.

The mean values of RSD of total SW and NE monsoon precipitation are shown in Figure 1. Throughout this article, raindrops below 1 mm and above 3 mm diameter are considered as small and large drops respectively. Raindrops from 1 to 3 mm diameter are considered as midsize drops. From the figure, it is clear that the mean RSD of small drops is less in SW monsoon compared to NE monsoon heavy precipitation; whereas the mean RSD of mid-size and large drops up to 4 mm have higher concentration in SW than NE monsoon. Large drops above 4 mm diameter have lower concentration in SW than NE monsoon.

The RSD measured with PARSIVEL disdrometer are stratified into 12 rainrate classes ($0.1 \le RR < 0.2$, $0.2 \le RR < 0.4$, $0.4 \le RR < 0.7$, $0.7 \le RR < 01$, $01 \le RR < 02$, $02 \le RR < 04$, $04 \le RR < 07$, $07 \le RR < 10$, $10 \le RR < 20$, $20 \le RR < 30$, $30 \le RR < 50$ and $RR \ge 50$). The
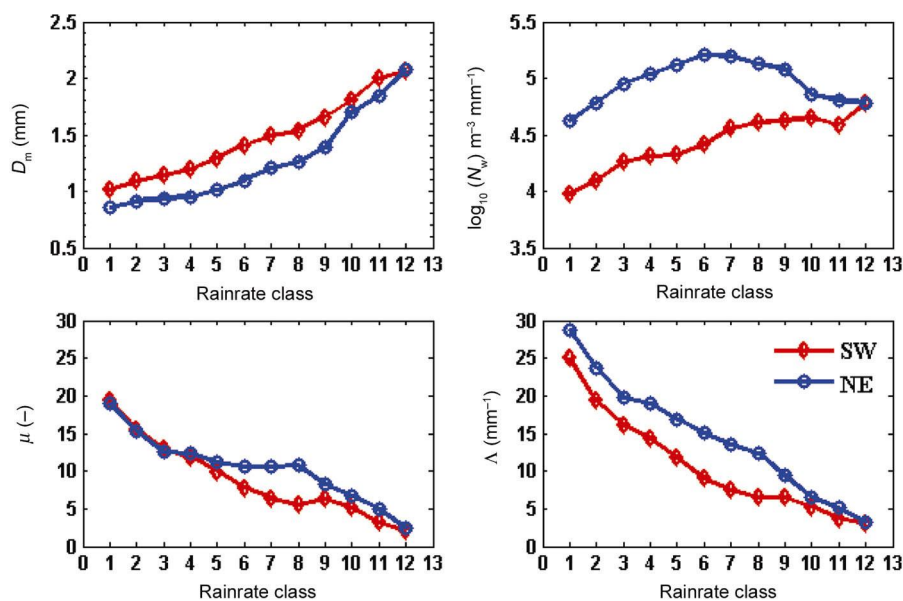
Figure 3. Variations in mean values of D_m, $\log_{10}(N_w)$, μ and Λ in each rainrate class of SW and NE monsoon precipitation.

rainrate classes are considered in such a way that mean value of each rainrate class is approximately equal in both the seasons. Rainrate statistics of SW and NE monsoon heavy rainfall are given in Table 1. From the table, it is observed that the mean value of each rainrate class is approximately equal in both the seasons except at RR ≥ 50 mm/h and each rainrate class has higher duration in SW than NE monsoon. The skewness is higher in SW than NE monsoon for light rainrate (RR < 02 mm/h) and is lower for rainrate above 2 mm/h. However, both the seasons have positive skewness. This means that most of the rainrate values are concentrated on left of the mean, with extreme values to the right. Both the seasons have kurtosis values less than 3 except at rainrate class greater than 50 mm/h. This implies that the distribution is flatter than a normal distribution with a wider peak. The probability for extreme values is less than that of a normal distribution, and the values are wider spread around the mean.

The RSD variations of SW and NE monsoon heavy precipitation in different rainrate classes are shown in Figure 2. The RSD concentration of small drops is higher in NE than SW monsoon for the rainrate classes of less than 20 mm/h, and for the rainrate above 20 mm/h, concentration in NE monsoon is either slightly higher or equal in magnitude. The difference in RSD concentration of small drops during SW and NE monsoon rainfall decreases with the increase in rainrate. The RSD concentration of mid-size drops is smaller in NE than SW monsoon for all the rainrate classes except for RR > 50 mm/h which is equal in both the seasons. For the large drops, no such consistent pattern is observed for both the seasons. The variation of small drop concentration in SW and NE monsoons

is similar to that observed by Rao et al.[4]. However, the variation in concentration of mid- and large-drops in SW and NE monsoons is different from that of the observations of Rao et al.[4].

To understand the RSD variability, SW and NE monsoon heavy precipitation RSDs are fitted to gamma function[19]. The variation of mass weighted mean diameter D_m (mm), normalized intercept parameter N_w (mm^{-1} mm^{-3}), shape μ (–) and slope parameter Λ (mm^{-1}) with rainrate class of SW and NE heavy precipitation are shown in Figure 3. It can be noticed from this figure that mean values of D_m are higher in SW than NE monsoon heavy precipitation in all the rainrate classes except at RR ≥ 50 mm/h. The mean value of D_m increases with the increase in rainrate class in both the seasons. This feature is consistent with the observations of other researchers[4,21]. The D_m value varied from 1.01 to 2.06 mm in SW monsoon and it ranges from 0.86 to 2.07 mm in NE monsoon heavy precipitation. The difference in mean D_m between SW and NE monsoon rainfall varied from 0.15 to 0.32 mm. This difference is smaller compared to the difference observed at Gadanki[4]. This variation in D_m difference between Gadanki and Kadapa may be due to local climate and topography around observational sites of Gadanki and Kadapa as well as different measuring principle of the (impact and laser) disdrometers[22]. The mean of normalized intercept parameter $\log_{10} N_w$ is higher in NE than SW monsoon in all the rainrate classes except at RR > 50 mm/h. The mean μ value is higher in SW monsoon for RR < 0.7 mm/h and is lower at above 0.7 mm/h than the near μ value for NE monsoon rainfall. In all the rainrate classes, mean value of slope parameter is lower for SW than NE monsoon. Mean values of D_m,
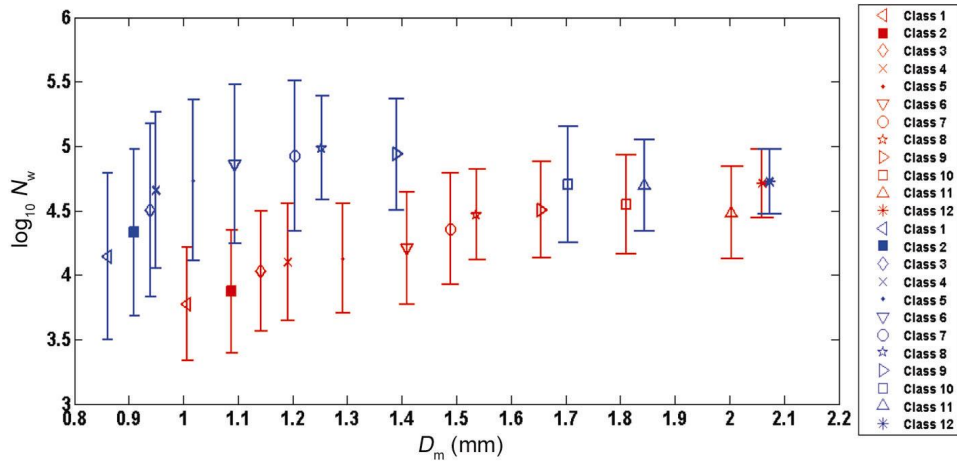
Figure 4. Mean and standard deviation of normalized intercept parameter ($\log_{10} N_w$) versus average mass weighted mean diameter (D_m) for convective and stratiform precipitation during SW and NE monsoon.

Table 3. Mean values of μ (dimensionless), Λ (mm^{-1}), D_m (mm) and N_t (m^{-3}) in the stratiform and convective precipitations of SW and NE monsoon precipitation

	Stratiform						Convective					
	D_m (mm)		$\log_{10}(N_w)$ (m^{-1} mm^{-3})		μ (–)	Λ (mm^{-1})	D_m (mm)		$\log_{10}(N_w)$ (m^{-1} mm^{-3})		μ (–)	Λ (mm^{-1})
Season	Mean	Standard	Mean	Standard	Mean	Mean	Mean	Standard	Mean	Standard	Mean	Mean
SW monsoon	1.250	0.297	3.990	0.402	10.212	12.843	1.237	0.446	4.159	0.603	13.347	16.215
NE monsoon	1.112	0.237	4.222	0.526	11.318	15.220	0.984	0.436	4.834	0.641	13.507	21.152

N_w, μ and Λ for SW and NE monsoon heavy precipitation at different rainrates are given in Table 2. Variation of mean values of $\log_{10} N_w$ (along with standard deviation) with the D_m for diffent rainrate classes in both the seasons is shown in Figure 4. The SW monsoon has larger D_m and smaller $\log_{10} N_w$ values in all the rainrate classes than NE monsoon rainfall. The difference in mean and standard deviation in $\log_{10} N_w$ between SW and NE monsoon seasons decreases with the increase in rainrate class.

Precipitation is generally considered to be divided into two distinct types: stratiform and convective. Identification of RSD features with these two precipitation types is useful and important for numerous applications[3,5]. Several rain classification schemes have been proposed by researchers[9,20,23] using different ground-based instruments such as disdrometer, profiler and radar. In this study, the SW and NE monsoon heavy precipitation is classified into stratiform and convective rainfall using MRR. If an enhanced reflectivity at the zero degree isotherm (bright band) is observed using MRR, then the corresponding rainfall is considered as stratiform; otherwise the rainfall is considered as convective. An example of the rainfall events (of 11 June 2010) classified as stratiform precipitation, showing a bright band is given in

Figure 5. The classification procedure assumes that stratiform rain tends to spread horizontally with fragile type of rain intensities, while convective system displays high intensities. The RSD of convective and stratiform rainfall observed during SW and NE monsoons are shown in Figure 6. In SW monsoon, a clear difference in raindrop concentration between convective and stratiform precipitations of all (small, midsize and large) raindrops can be seen. In the NE monsoon, small drops have less difference in raindrop concentration; whereas midsize and large drops have large difference in drop concentration between convective and stratiform precipitation. Small and large drops in SW monsoon stratiform precipitation have less drop concentration than NE monsoon stratiform precipitation. Midsize drops in SW stratiform precipitation have higher concentration in SW than NE stratiform precipitation. Convective precipitations of both SW and NE monsoon seasons have nearly equal raindrop concentration for all (small, midsize and large) raindrops. This suggests that the RSD difference between both the seasons is mainly due to the differences in RSD of stratiform rather than convective precipitation.

Mean values of $\log_{10} N_w$ (mm^{-1} mm^{-3}), D_m (mm), μ (–) and Λ (mm^{-1}) of stratiform and convective precipitations of both the seasons are given in Table 3. It is apparent
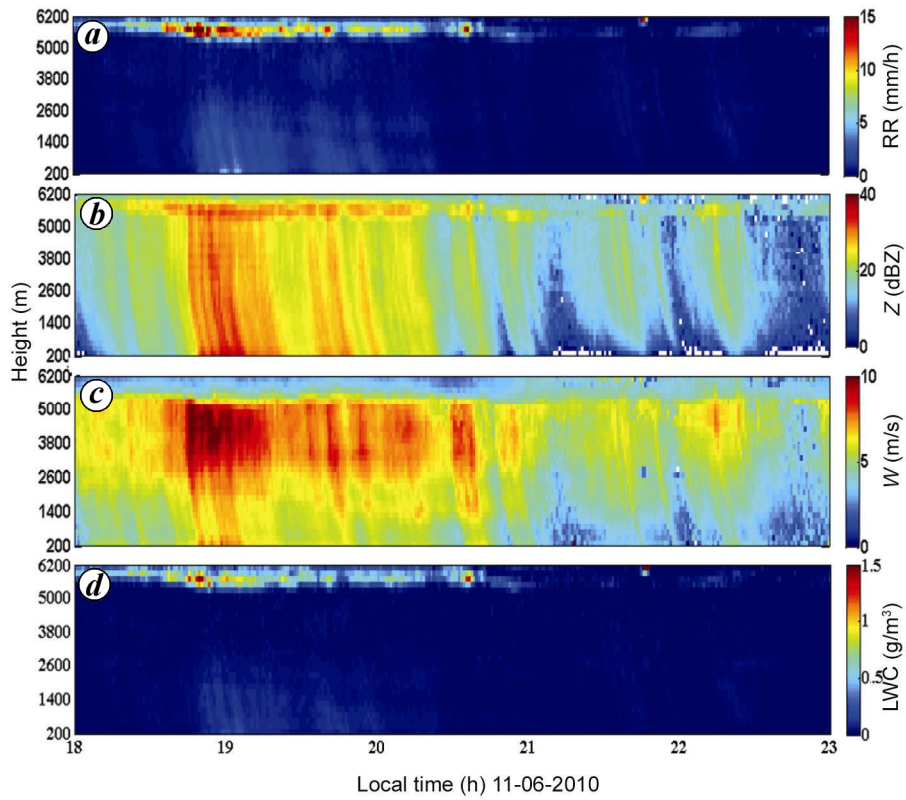
Figure 5. Time–height cross-section of (*a*) rainrate (RR) (mm/h), (*b*) radar reflectivity *Z* (dBZ), (*c*) fall velocity *w* (m/s), (*d*) liquid water content (LWC) (g/m^3) of the stratiform cloud fraction from a precipitating cloud observed on 11 June 2011.
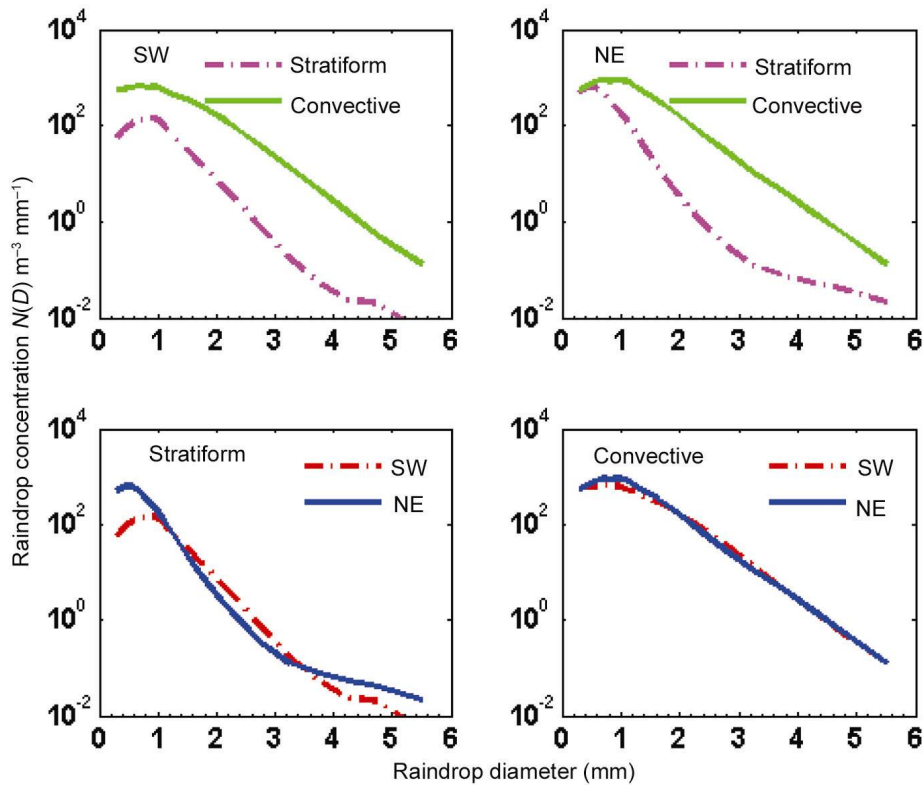
Figure 6. Rate size distribution of SW and NE monsoon heavy precipitation in stratiform and convective regimes.

Table 4. Z–R relations for different seasons and precipitations for Kadapa and Gadanki locations

Location	Kadapa	Gadanki
Season/type of precipitation	$Z = A * R^b$	$Z = A * R^b$
SW monsoon	$Z = 300.500 * R^{1.375}$	$Z = 407.00 * R^{1.32}$ (ref. 23)
		$Z = 264.30 * R^{1.468}$ (ref. 3)
		$Z = 293.18 * R^{1.441}$ (ref. 4)
NE monsoon	$Z = 163.324 * R^{1.350}$	$Z = 155.00 * R^{1.39}$ (ref. 23)
		$Z = 72.30 * R^{1.697}$ (ref. 3)
		$Z = 186.43 * R^{1.549}$ (ref. 4)
SW monsoon stratiform	$Z = 334.132 * R^{1.424}$	$Z = 251 * R^{1.48}$ (ref. 23)
NE monsoon stratiform	$Z = 245.349 * R^{1.283}$	
SW monsoon convective	$Z = 265.586 * R^{1.341}$	$Z = 178 * R^{1.51}$ (ref. 23)
NE monsoon convective	$Z = 122.407 * R^{1.430}$	
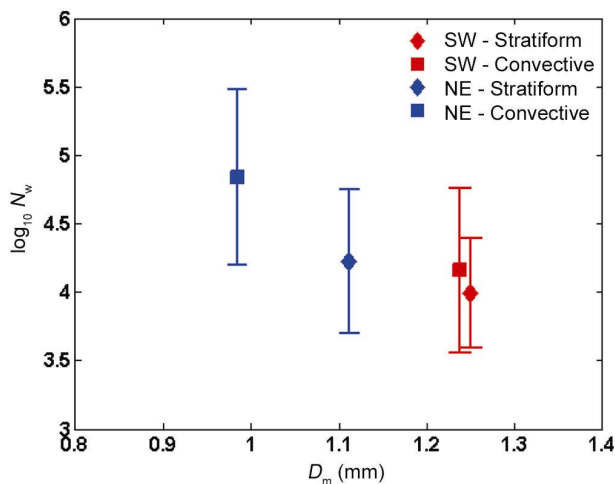
Figure 7. Mean and standard deviation of normalized intercept parameter ($\log_{10} N_w$) versus average mass weighted mean diameter (D_m) for convective and stratiform precipitation of SW and NE monsoon seasons.
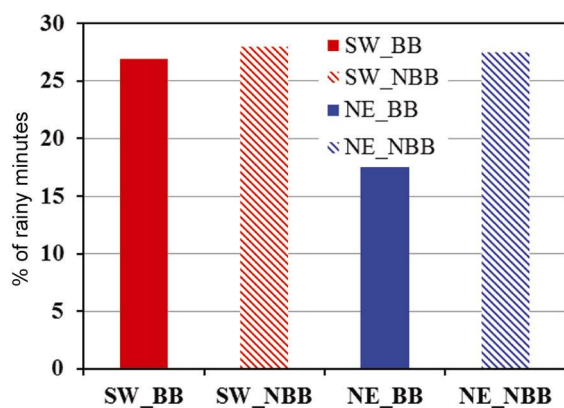
Figure 8. Percentage occurrence (duration in minutes) of bright band (BB) and no bright band (NBB) of SW and NE monsoon.

that for both the seasons, the mean D_m value is higher in stratiform than convective precipitation; whereas the mean value of $\log_{10} N_w$ is higher in convective than strati-

form precipitation in both the seasons. Both stratiform and convective precipitations of SW monsoon are associated with higher D_m values and smaller $\log_{10} N_w$ values than NE monsoon precipitations. The slope and shape parameters are higher in both the precipitations (stratiform and convective) of NE than SW monsoon. The convective precipitations of both the seasons are associated with higher μ and Λ values than stratiform precipitation. Variation of mean and standard deviation of $\log_{10} N_w$ with D_m for convective and stratiform precipitations of SW and NE monsoon seasons is given in Figure 7. The stratiform precipitation of SW and NE monsoon seasons is associated with higher D_m and lower $\log_{10} N_w$ values; and their corresponding convective precipitations are associated with lower D_m and higher $\log_{10} N_w$ values. These results are consistent with different microphysical formation mechanics involved in the stratiform (large D_m and smaller $\log_{10} N_w$) and convective (small D_m and large $\log_{10} N_w$) precipitation classification suggested by Bringi et al.[20]. Stratiform precipitation is associated with melting of large dry snowflakes, whereas convective precipitation is associated with melting of tiny graupel or smaller rimed ice particles. However, both convective and stratiform precipitations of SW monsoon are associated with higher D_m and lower $\log_{10} N_w$ values than NE monsoon. This may be due to the persistence of stratiform precipitation for longer duration in SW than NE monsoon and this can be ascertained from Figure 8. This figure clearly shows the occurrence of higher percentage of stratiform precipitation and a slightly higher convective precipitation in SW monsoon than NE monsoon.

Differences in RSD for different seasons and types of precipitation may lead to different Z–R relations. If a single Z–R relation is used for different locations, there is a possibility of underestimation or overestimation of rain-rates with the weather radars. Hence, in this study, present work radar reflectivity (Z) and rainrate (R) relations are obtained for SW and NE monsoon seasons as well as for stratiform and convective types of rainfall over Kadapa. The coefficient A and exponent b of SW and NE monsoon rainfall as well as their corresponding stratiform

and convective rainfall are given in Table 4. The coefficient A and exponent b are higher in SW than NE monsoon. However, Gadanki and other researchers[3,4,23] reported that the coefficient A is higher and exponent b is lower in SW than NE monsoon. In both convective and stratiform precipitations, SW monsoon has higher coefficient (A) values than NE monsoon. In both the seasons, coefficient A is larger for stratiform than convective precipitation. Similar type of observational results have been obtained by Kozu *et al.*[3] and Rao *et al.*[4].

A field experiment was conducted at Kadapa located in a region of tropical, continental, semi-arid climate. A total of 15,588 min raindrop size distributions measured with a PARSIVEL disdrometer and MRR is analysed to discern the similarity and difference between stratiform and convective rains, to determine the statistical pattern of the raindrop size distribution during SW and NE monsoon heavy precipitation. The RSD stratified on the basis of rainrate showed that the concentration of small drops is less in SW than NE monsoon precipitation and a reverse pattern is observed for midsize drops. In both the seasons, the mass weighted mean diameter (D_m) increases with increase in rainrate class. The RSD fitted to gamma function showed that mean value of mass weighted mean diameter, D_m is higher and normalized intercept parameter $\log_{10} N_w$ is lower in SW than NE monsoon. In the entire rainrate classes, SW monsoon rainfall is associated with larger D_m and smaller $\log_{10} N_w$ values compared to that of NE monsoon rainfall. The rainfall classification done with MRR showed a clear difference in RSD between convective and stratiform precipitations of SW and NE monsoon seasons. Both the seasons have similar RSD concentration in convective precipitation. However, there is difference in RSD concentration of stratiform precipitation of both the seasons. Radar reflectivity and rainrate ($Z–R$) relations are derived for seasons as well as types of precipitation. The coefficient A and exponent b are higher in SW than NE monsoon. In both the seasons, the coefficient A is larger for stratiform than convective precipitation.

1. Tenório, R. S., da Silva Moraes, M. C. and Sauvageot, H., Raindrop size distribution and radar parameters in coastal tropical rain systems of northeastern Brazil. *J. Appl. Meteorol. Climatol.*, 2012, **51**(11), 1960–1970.
2. Reddy, K. K. and Kozu, T., Measurements of raindrop size distribution over Gadanki during southwest and northeast monsoon. *Indian J. Radio Space Phys.*, 2003, **32**, 286–295.
3. Kozu, T., Reddy, K. K., Mori, S., Thurai, M., Ong, J. T., Rao, D. N. and Shimomai, T., Seasonal and diurnal variations of raindrop size distribution in Asian monsoon region. *J. Meteorol. Soc. Jpn.*, 2006, **84A**, 195–209.
4. Rao, T. N., Radhakrishna, B., Nakamura, K. and Rao, N. P., Differences in raindrop size distribution from southwest monsoon to northeast monsoon at Gadanki. *Q. J. R. Meteorol. Soc.*, 2009, **135**, 1630–1637.
5. Maki, M., Keenan, T. D., Sasaki, Y. and Nakamura, K., Characteristics of the raindrop size distribution in tropical continental squall lines observed in Darwin, Australia. *J. Appl. Meteorol.*, 2001, **40**, 1393–1412.
6. Friedrich, K., Kalina, E. A., Masters, F. J. and Lopez, C. R., Drop-size distributions in thunderstorms measured by optical disdrometers during VORTEX2. *Mon. Wea. Rev.*, 2013, **141**, 1182–1203.
7. Balaji Kumar, S., Krishna Reddy, K., Murali Krishna, U. V. and Pathak, H. G., A new algorithm for classification of tropical convective precipitating clouds observed over north eastern region of India. *IJAET*, 2013, **6**(1), 405–414.
8. Reddy, K. K., Kozu, T., Ohno, Y., Jain, A. R. and Rao, D. N., Estimation of vertical profiles of raindrop size distribution from the VHF wind profiler radar Doppler spectra. *Indian J. Radio Space Phys.*, 2005, **34**, 319–327.
9. Tokay, A. and Short, D. A., Evidence of tropical raindrop spectra of the origin of rain from stratiform versus convective clouds. *J. Appl. Meteorol. Clim.*, 1996, **35**, 355–371.
10. Niu, S., XingcanJia, Sang, J., Liu, X., Lu, C. and Liu, Y., Distributions of raindrop sizes and fall velocities in a semiarid plateau climate: convective versus stratiform rains. *J. Appl. Meteorol. Climatol.*, 2010, **49**, 632–645.
11. Chakravari, K. and Raj, P. E., Raindrop size distributions and their association with characteristics of clouds and precipitation during monsoon and post-monsoon periods over a tropical Indian station. *Atmos. Res.*, 2013, **124**, 181–189.
12. Harikumar, R., Sampath, S. and Kumar, V. S., Variation of rain drop size distribution with rain rate at a few coastal and high altitude stations in southern peninsular India. *Adv. Space Res.*, 2010, **45**, 576–586.
13. Radhakrishna, B. and Rao, T. N., Differences in cyclonic raindrop size distribution from southwest to northeast monsoon season and from that of noncyclonic rain. *J. Geophys. Res.-Atmos.*, 2010, **115**, D16205; doi: 10.1029/2009JD013355.
14. Balaji Kumar, S. and Krishna Reddy, K., Raindrop size distribution characteristics of cyclonic and north east monsoon thunderstorm precipitating clouds observed over Kadapa (14.47°N, 78.82°E), tropical semi-arid region of India. *Mausam*, 2013, **64**(1), 35–48.
15. Loffler-Mang, M. and Joss, J., An optical disdrometer for measuring size and velocity of hydrometeors. *J. Atmos. Ocean. Technol.*, 2000, **17**, 130–139.
16. Peters, G., Fischer, B. and Andersson, T., Rain observation with a vertically looking Micro Rain Radar (MRR). *Boreal Environ. Res.*, 2002, **7**, 353–362.
17. Cha, J. W., Yum, S. S., Chang, K. H. and Oh, S. N., Estimation of the melting layer from a Micro Rain Radar (MRR) data at the cloud physics observation system (CPOS) site at Daegwallyeong Weather Station. *J. Kor. Meteorol. Soc.*, 2007, **43**(1), 77–85.
18. Löffler-Mang, M. and Kunz, M., On the performance of a low-cost K-band Doppler radar for quantities rain measurements. *J. Atmos. Ocean. Technol.*, 1999, **16**, 379–387.
19. Ulbrich, C. W., Natural variations in the analytical form of the raindrop size distribution. *J. Clim. Appl. Meteorol.*, 1983, **22**(10), 1764–1775.
20. Bringi, V. N., Chandrasekar, V., Hubbert, J., Gorgucci, E., Randeu, W. L. and Schoenhuber, M., Raindrop size distribution in different climatic regimes from disdrometer and dual-polarized radar analysis. *J. Atmos. Sci.*, 2003, **60**, 354–365.
21. Rosenfeld, D. and Ulbrich, C. W., Cloud microphysical properties, processes, and rainfall estimation opportunities. *Meteorol. Monogr.*, 2003, **30**(52), 237–258.
22. Thurai, M., Petersen, W. A., Tokay, A., Schultz, C. and Gatlin, P., Drop size distribution comparisons between Parsivel and 2-D video disdrometers. *Adv. Geosci.*, 2011, **30**, 3–9.
23. Rao, T. N., Rao, D. N., Mohan, K. and Raghavan, S., Classification of tropical precipitating systems and associated $Z–R$ relationships. *J. Geophys. Res.*, 2001, **106**, 17699–17711.